M-band filtering and nonredundant directional wavelets

Sylvain Durand

M-band Filtering and Non-redundant Directional Wavelets

Sylvain Durand
LAMFA UMR 6140–Université de Picardie 33 rue Saint-Leu, 90039 Amiens Cedex
CMLA UMR 8536–ENS de Cachan, 61 av. du Président Wilson, 94235 Cachan Cedex
e-mail: sdurand@cmla.ens-cachan.fr

Abstract

This article introduces families of nonadaptive directional wavelets. Unlike curvelets and contourlets, they are non-redundant and form orthonormal bases for $L^2(\mathbb{R}^2)$. Their implementation derives from a single nonseparable filter bank structure with non-uniform sampling. We give several examples of frequency partitioning, including constructions based on separable multiresolution analyses. We show how to obtain orthonormal bases of wavelets with fast decay, and compactly supported, biorthogonal wavelet bases. Some aliasing phenomena that can occur in these constructions are discussed.

1 Introduction

In some signal and image processing applications such as compression and denoising, one is led to search for sparse representations. For instance, the wavelet transform is very popular as it provides good non-linear approximations of peacewise smooth signals. Wavelet basis on $\mathbb{R}^2$ are generally obtained by tensor product, but separable wavelets are not well suited to images that have discontinuities positioned along regular curves. In order to capture geometrical structures of images, many authors proposed new transformations as natural extensions of wavelets on $\mathbb{R}^2$. Some approaches consist in adapting separable wavelets to the structures of each image. For example, bandelets [11] are obtained by warping wavelets along the geometrical flow of the image. Some authors considered however nonadaptive transformations. Although representations of images by such transformations may be less sparse, the algorithms are generally faster. Moreover, no bits are wasted in the description of the geometry, when dealing with compression.

Due to its high directionality, the curvelet frame introduced by Candès and Donoho [3], provides an optimal approximation of piecewise smooth images with C^2 edges. Originally developed in the continuous case, the curvelets are, however, difficult to implement on discrete images. In order to circumvent this problem, Do and Vetterli [7] introduced the contourlets that have the same geometry as curvelets but are directly defined on a discrete lattice. Although they perform very well in low bit rate compression, contourlets are still redundant frames (with redundancy factor 1.33) that make them non adapted to hight bit rate and lossless compression. Lu and Do [12] introduced a directional filter bank that provides a frequency partitioning which is close to the curvelets' but with no redundancy. It consists in splitting the image on

four directional subbands and then applying a multiscaling algorithm on each band. Although it has the same geometry as one of the examples we consider below (Example B), this construction does not derives from a multiresolution analysis (MRA) of $L^2(\mathbb{R}^2)$ which vouches for the obtaining of a basis for $L^2(\mathbb{R}^2)$. The same frequency partitioning was studied very recently by Nguyen and Oraintara [17]. The proposed transformation is based on a non-uniform filter bank as it is the case for the transformations considered in this article. But the filters are obtained by an optimization method that ensures approximate reconstruction only.

Several other transformations have been proposed. All of these approaches emphasize the difficulty to have simultaneously non-redundancy (it fails for [3, 7, 10]), sharp directionality (see [10, 13]), space localization (see [2, 10]) and an easy implementation (see [2, 3]) with a natural relation between continuous and discrete cases (see [9, 12]).

The aim of this article is to develop ideas introduced in a short article [8] in order to meet these objectives. The transformation we proposed is generated by an MRA. It uses a single filter bank structure with non-uniform sampling. In section 2, we gives a condition for perfect reconstruction non-uniform filter banks. In Section 3, we focus on Shannon filters in order to define the ideal frequency supports of directional wavelets. Several examples are considered. Section 4 is devoted to the design of some specific two-band filters that are used in the next sections. Three examples of frequency partitionings are studied in more details, in the last sections. We construct smooth approximations of Shannon filters in order to obtain orthogonal wavelets with fast decay and compactly supported biorthogonal wavelets. The problem of aliasing that appears in some constructions is also adressed.

2 M-band filtering with non-uniform sampling

Denote by $\|\,.\,\|$ the Euclidean norm and by $\langle\,.\,,\,.\,\rangle$ the scalar product on $\mathbb{R}^n$. Given $(e_k)_{k=1}^n$ a basis for $\mathbb{R}^n$, one defines a point lattice by

$$\Gamma = \sum_{k=1}^{n} \mathbb{Z}\, e_k.$$

Its reciprocal lattice is defined by

$$\Gamma^* = \{\gamma \in \mathbb{R}^n : \langle \eta, \gamma \rangle \in 2\pi\mathbb{Z},\ \forall \eta \in \Gamma\},$$

so that the Fourier transformation is an isometry between $l^2(\Gamma)$ and $L^2(\mathbb{R}^n/\Gamma^*)$. For two lattices Γ_1 and Γ_2 with $\Gamma_2 \subset \Gamma_1$, define also the quotient lattice $\Gamma_1/\Gamma_2 = \{\overline{\gamma} : \gamma \in \Gamma_1\}$, where $\overline{\gamma} = \{\delta \in \Gamma_1 :\ \delta - \gamma \in \Gamma_2\}$. Denote by $|E|$ the cardinal number of any set E.

Given an original lattice $\Lambda \subset \mathbb{R}^n$, a filter bank $((M_k, \widetilde{M}_k)_{k\in K}, D)$ is defined by transfer functions $(M_k)_{k\in K}$ and $(\widetilde{M}_k)_{k\in K}$ in $L^2(\mathbb{R}^n/\Lambda^*)$, and a subsampling map D. The latter must preserve the lattice Λ in the sense that it satisfies the condition $\Gamma = D\Lambda \subset \Lambda$. The original signal $x \in l^2(\Lambda)$ is filtered on $|K|$ subbands using the transfer functions $(\overline{M_k})_{k\in K}$ where $\overline{M_k}(\xi)$ stands for the complex conjugate of $M_k(\xi)$. Subbands are next subsampled on the common lattice Γ. At reconstruction, the subband of index k is resampled on Λ by adding zeroes and filtered using the transfer function $\widetilde{M}_k$. The $|K|$ obtained filtered signal are added in order to generate the

reconstructed signal $\widetilde{x}$. One says that the filter bank performs a perfect reconstruction if and only if $x = \widetilde{x}$.

Notice that, at this point, the choice of the subsampling map D is not fundamental (one only needs to know $\Gamma = D\Lambda$). It interferes only when the filter bank is reiterated on, at least, one of the subbands as it is the case for wavelets. For simplicity, this choice will remain indeterminate (although it will be clear in the constructions below). We will use therefore the notation $((M_k, \widetilde{M_k})_{k\in K}, \Lambda \to \Gamma)$ instead of $((M_k, \widetilde{M_k})_{k\in K}, D)$.

A necessary and sufficient condition for perfect reconstruction [19] is that

$$M(\xi)^* \, \widetilde{M}(\xi) = |\Lambda/\Gamma| \, \mathrm{Id}_{|\Lambda/\Gamma|}, \tag{1}$$

for *a.e.* $\xi \in \mathbb{R}^2$, where $M(\xi) = (M_k(\xi+\gamma))_{\gamma\in\Gamma^*/\Lambda^*;\, k\in K}$, $\widetilde{M}(\xi) = (\widetilde{M_k}(\xi+\gamma))_{\gamma\in\Gamma^*/\Lambda^*;\, k\in K}$, $M(\xi)^*$ is the conjugate transpose of the matrix $M(\xi)$ and $\mathrm{Id}_{|\Lambda/\Gamma|}$ is the $|\Lambda/\Gamma| \times |\Lambda/\Gamma|$-identity matrix. A simple way to show this result is to express the Fourier transform of the reconstructed signal $\widetilde{x}$ as

$$\widehat{\widetilde{x}} = \frac{1}{|\Lambda/\Gamma|} \sum_{k\in K} \overline{M_k} \, \widetilde{M}_k \, \widehat{x} + \frac{1}{|\Lambda/\Gamma|} \sum_{\gamma\in(\Gamma^*/\Lambda^*)\setminus\{0\}} \sum_{k\in K} \overline{M_k}(\,.\,+\gamma) \, \widetilde{M}_k \, \widehat{x}(\,.\,+\gamma).$$

Condition (1) means that the first term on the right hand side is equal to $\widehat{x}$, the Fourier transform of the original signal x, while the other terms vanish. For example, $((e^{i\langle\eta,\,.\,\rangle}, e^{i\langle\eta,\,.\,\rangle})_{\eta\in\Lambda/\Gamma}, \Lambda \to \Gamma)$ performs a perfect reconstruction. It amounts, indeed, to subsample the original signal on the shifted lattices $\{\Gamma + \eta\}_{\eta\in\Lambda/\Gamma}$ whose union is the whole lattice Λ.

More generally, let us assume that the subbands are subsampled on different lattices $\{\Gamma_k\}_{k\in K}$ with $\Gamma_k \subset \Lambda$, for all $k \in K$. Denote by Γ a common sublattice of all the lattices Γ_k. (In other words, one has $\Gamma \subset \Gamma_k$, $\forall k \in K$. Notice that such a lattice Γ exists because $\Gamma_k \subset \Lambda$, $\forall k \in K$.) Define

$$M(\xi) = \Big(e^{i\langle\eta_k,\xi+\gamma\rangle} \, M_k(\xi+\gamma)\Big)_{\gamma\in\Gamma^*/\Lambda^*;\, k\in K,\, \eta_k\in\Gamma_k/\Gamma},$$

and

$$\widetilde{M}(\xi) = \Big(e^{i\langle\eta_k,\xi+\gamma\rangle} \, \widetilde{M}_k(\xi+\gamma)\Big)_{\gamma\in\Gamma^*/\Lambda^*;\, k\in K,\, \eta_k\in\Gamma_k/\Gamma}.$$

Then we have the following reconstruction result

Proposition 1 *The filter bank $(M_k, \widetilde{M_k}, \Lambda \to \Gamma_k)_{k\in K}$ performs a perfect reconstruction if and only if*

$$M(\xi)^* \, \widetilde{M}(\xi) = |\Lambda/\Gamma| \, Id_{|\Lambda/\Gamma|} \tag{2}$$

for a.e. $\xi \in \mathbb{R}^n$.

Proof. Equation (2) amounts to say that the filter bank defined by the transfer functions $(e^{i\langle\eta_k,\,.\,\rangle} \, M_k, \, e^{i\langle\eta_k,\,.\,\rangle} \, \widetilde{M_k})_{k\in K,\, \eta_k\in\Gamma_k/\Gamma}$ and the common subsampling lattice Γ, performs a perfect reconstruction. The latter can however be seen as a combination of $(M_k, \widetilde{M_k}, \Lambda \to \Gamma_k)_{k\in K}$ and the filter banks $((e^{i\langle\eta,\,.\,\rangle}, e^{i\langle\eta,\,.\,\rangle})_{\eta\in\Gamma_k/\Gamma}, \Gamma_k \to \Gamma)$ that are applied to the subbands of index k respectively. The proof derives from the fact that filter banks $((e^{i\langle\eta,\,.\,\rangle}, e^{i\langle\eta,\,.\,\rangle})_{\eta\in\Gamma_k/\Gamma}, \Gamma_k \to \Gamma)$ perform perfect reconstructions. $\diamond$

In the sequel, in order to obtain non-redundant transformations, we assume that $\sum_{k\in K} |\Gamma_k/\Gamma| = |\Lambda/\Gamma|$. This condition means that the matrix $M(\xi)$ is square.

3 Admissible frequency partitioning

We consider, in this section, the special case of filter banks and wavelets which have ideal localization in the Fourier domain, in the sense that the transfer function of the filters and the Fourier transforms of the wavelets are indicator functions. These wavelets, known as Shannon wavelets, suffer a bad localization in the space domain since they do not belong to $L^1(\mathbb{R}^2)$. Their study is motivated by the design of the ideal frequency partitioning that we will try to approximate. In the next sections, we show how to obtain a better space localization. A first step consists in characterizing the admissible partitions for filter banks, as they are defined below.

One calls partition or set partition of $\mathbb{R}^n$, a collection of disjoint subsets of $\mathbb{R}^n$ whose union is $\mathbb{R}^n$. A family of sets $\{A_k\}_{k\in K}$ is said to be a partition of $\mathbb{R}^n/\Lambda^*$ if and only if $\{A_k + \Lambda^*\}_{k\in K}$ is a partition of $\mathbb{R}^n$. For convenience, sets are defined modulo a set of Lebesgue measure zero. Given a lattice $\Lambda \subset \mathbb{R}^n$, a reciprocal cell is a set $\mathcal{C} \subset \mathbb{R}^n$ such that $(\mathcal{C} + \{\gamma\})_{\gamma\in\Lambda^*}$ is a partition of $\mathbb{R}^n$. We consider only Voronoi reciprocal cells $\mathcal{C}$ defined by $\xi \in \mathcal{C} \Rightarrow \|\xi\| \leq \|\xi + \gamma\|$, $\forall \gamma \in \Lambda^*$. Let us denote by χ_E the indicator function of a set E.

Definition 1 *A partition $\{A_k\}_{k\in K}$ is said to be* admissible *if and only if there exist lattices $\Lambda \subset \mathbb{R}^n$ and $\Gamma_k \subset \Lambda$, $\forall k \in K$, such that the filter bank $(M_k, \widetilde{M}_k, \Lambda \to \Gamma_k)_{k\in K}$ defined by*

$$M_k = \widetilde{M}_k = \sqrt{|\Lambda/\Gamma_k|}\, \chi_{A_k+\Lambda^*}, \quad \forall k \in K, \tag{3}$$

performs a perfect reconstruction

Proposition 2 *The partition $\{A_k\}_{k\in K}$ is admissible if and only if there exist lattices $\Lambda \in \mathbb{R}^n$ and $\Gamma_k \subset \Lambda$, $\forall k \in K$, such that*

$$\{A_k\}_{k\in K} \quad \textit{is a partition of } \mathbb{R}^n/\Lambda^*, \tag{4}$$

and

$$\{A_k + \gamma\}_{\gamma\in\Gamma_k^*/\Lambda^*} \quad \textit{is a partition of } \mathbb{R}^n/\Lambda^*, \quad \forall k \in K. \tag{5}$$

Proof. On one hand, Condition (4) implies that, for *a.e.* $\xi \in \mathbb{R}^n$,

$$\begin{aligned}
\sum_{k\in K} \sum_{\eta_k\in\Gamma_k/\Gamma} \overline{e^{i\langle\eta_k,\xi\rangle}\, M_k(\xi)}\, e^{i\langle\eta_k,\xi\rangle}\, \widetilde{M}_k(\xi) &= \sum_{k\in K} \sum_{\eta_k\in\Gamma_k/\Gamma} \left(\sqrt{|\Lambda/\Gamma_k|}\, \chi_{A_k+\Lambda^*}(\xi)\right)^2 \\
&= \sum_{k\in K} |\Gamma_k/\Gamma|\, |\Lambda/\Gamma_k|\, \chi_{A_k+\Lambda^*}(\xi) \\
&= |\Lambda/\Gamma|.
\end{aligned}$$

On the other hand, Condition (5) implies that $\chi_{A_k}(\xi)\, \chi_{A_k}(\xi + \gamma_k) = 0$, for all $k \in K$ and $\gamma_k \in \Gamma_k^*$, which leads to

$$\sum_{k\in K} \sum_{\eta_k\in\Gamma_k/\Gamma} \overline{e^{i\langle\eta_k,\xi\rangle}\, M_k(\xi)}\, e^{i\langle\eta_k,\xi+\gamma_k\rangle}\, \widetilde{M}_k(\xi + \gamma_k) = 0.$$

By Proposition 1, $(M_k, \widetilde{M}_k, \Gamma_k)_{k\in K}$ performs therefore a perfect reconstruction. Conversely, if equation (2) is satisfied, one obtains by the same calculation as above,

$$\sum_{k\in K} \left(\chi_{A_k+\Lambda^*}(\xi)\right)^2 = 1,$$

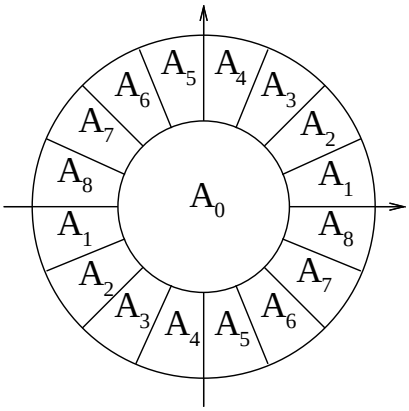

Figure 1: No lattice corresponds to this ideal frequency partitioning.

which proves (4). Similarly,

$$\sum_{\gamma\in\Gamma^*/\Lambda^*} \overline{e^{i\langle\eta_k,\xi+\gamma\rangle}\, M_k(\xi+\gamma)}\, e^{i\langle\eta_k,\xi+\gamma\rangle}\, \widetilde{M}_k(\xi+\gamma) = |\Lambda/\Gamma|, \quad \forall k\in K,\, \forall \eta_k\in\Gamma_k,$$

proves that

$$\sum_{\gamma\in\Gamma_k^*/\Lambda^*} \left(\chi_{A_k+\Lambda^*}(\xi+\gamma)\right)^2 = 1, \quad \forall k\in K,$$

which leads to (5). ◇

The wavelets that are considered in this article derive from an MRA. The notation M_0 is assigned to the refinement filter. We require henceforth that 0 belongs to the interior of A_0. Moreover, we require M_0 to be as much isotropic as possible in the sense that the set A_0 satisfies some invariance by rotation property. There are mainly two possible choices: square or hexagonal shape.

In order to have filters with real coefficients, and consequently to have real valued wavelets, we require the sets A_k to be symmetric with respect to 0. For instance, when $n=2$, given an original lattice $\Lambda\subset\mathbb{R}^2$ with reciprocal cell $\mathcal{C}$, put

$$A_k = \{\xi\in\mathcal{C}\setminus A_0 :\ \text{Arctan}\ \xi_2/\xi_1 \in [\theta_{k-1},\theta_k]+\pi\mathbb{Z}\},$$

for some parameters $(\theta_k)_{k\in K}$ (see Figure 1). Clearly, $\{A_k\}_{k\in K}$ is a partition of $\mathcal{C}$. The question is therefore to find A_0, $(\theta_k)_{k\in K}$ and $(\Gamma_k)_{k\in K}$ such that the partition $\{A_k,\Gamma_k\}_{k\in K}$ is admissible, or equivalently, the families $\{A_k+\gamma\}_{\gamma\in\Gamma^*/\Lambda^*}$ form partitions of $\mathbb{R}^2/\Lambda^*$, for all $k\in K$. We give here examples on $\mathbb{R}^2$ although the study could be generalized to $\mathbb{R}^n$.

Example A Let $\Lambda=\mathbb{Z}^2$. Then we have $\mathcal{C}=[-\pi,\pi]^2$. Consider the case of quincunx MRA where the refinement filter is defined by the set

$$A_0 = \{\xi\in\mathbb{R}^2 :\ |\xi_1-\xi_2|<2\pi \ \text{ and } \ |\xi_1-\xi_2|<2\pi\}.$$

The associated sublattice is

$$\Gamma_0 = \begin{pmatrix} 1 & 1 \\ 1 & -1 \end{pmatrix}\mathbb{Z}^2.$$

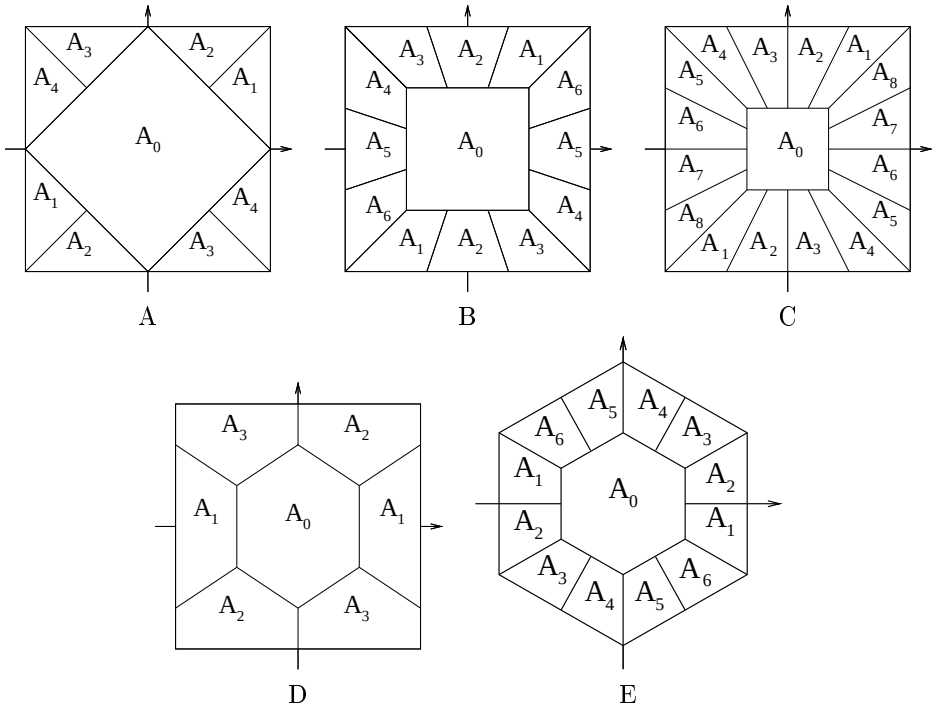

Figure 2: Examples of admissible frequency partitionings.

The quincunx Shannon wavelet corresponds to the case of 1 direction. More precisely, we have $A_1 = [-\pi,\pi]^2 \setminus A_0$ and $\Gamma_1 = \Gamma_0$. One can however obtain 2 directions by putting $\theta_k = k\pi$ and $\Gamma_k = 2\,\mathbb{Z}^2$, or 4 directions with $\theta_k = k\pi/2$ and $\Gamma_k = 2\,\Gamma_0$ (see Figure 2–A).

Example B Let $\Lambda = \mathbb{Z}^2$ and consider the well-known case of a separable, dyadic MRA. We have $A_0 = [-\pi/2,\pi/2]^2$ and $\Gamma_0 = 2\,\mathbb{Z}^2$. We can have $6p$ directions (with $p \in \mathbb{N} \setminus \{0\}$). For instance, if $p = 1$, put

$$\begin{array}{rcl} A_1 & = & \{\xi \in [-\pi,\pi]^2 \setminus A_0 :\ \xi_1 \le \xi_2 \le 3\xi_1 \text{ or } 3\xi_1 \le \xi_2 \le \xi_1\} \\ A_2 & = & \{\xi \in [-\pi,\pi]^2 \setminus A_0 :\ 3|\xi_1| \le \xi_2 \text{ or } \xi_2 \le 3|\xi_1|\} \\ A_3 & = & \{\xi \in [-\pi,\pi]^2 \setminus A_0 :\ (-\xi_1,\xi_2) \in A_1\} \\ A_4 & = & \{\xi \in [-\pi,\pi]^2 \setminus A_0 :\ (\xi_2,\xi_1) \in A_1\} \\ A_5 & = & \{\xi \in [-\pi,\pi]^2 \setminus A_0 :\ (\xi_2,\xi_1) \in A_2\} \\ A_6 & = & \{\xi \in [-\pi,\pi]^2 \setminus A_0 :\ (\xi_2,\xi_1) \in A_3\} \end{array} \tag{6}$$

These sets are shown on Figure 2–B. The 6 wavelets subbands are sampled on the same lattice

$$\Gamma = 2 \begin{pmatrix} 1 & -1 \\ 1 & 1 \end{pmatrix} \mathbb{Z}^2, \tag{7}$$

with reciprocal lattice

$$\Gamma^* = \frac{\pi}{2} \begin{pmatrix} 1 & -1 \\ 1 & 1 \end{pmatrix} \mathbb{Z}^2. \tag{8}$$

One checks easily that each set A_k can be split in p subsets in order to obtain more

directions (see Figure 3–B). The $6p$ wavelets subbands are sampled on the lattices

$$\begin{cases} \Gamma_k = \begin{pmatrix} 4 & 2p \\ 0 & 2p \end{pmatrix} \mathbb{Z}^2, & \text{if } k \in \{1, \ldots, 3p\}, \\ \Gamma_k = \begin{pmatrix} 2p & 0 \\ 2p & 4 \end{pmatrix} \mathbb{Z}^2, & \text{if } k \in \{3p+1, \ldots, 6p\}. \end{cases}$$

The latters correspond to the reciprocal lattices

$$\begin{cases} \Gamma_k^* = \begin{pmatrix} \pi/2 & 0 \\ -\pi/2 & \pi/p \end{pmatrix} \mathbb{Z}^2, & \text{if } k \in \{1, \ldots, 3p\}, \\ \Gamma_k^* = \begin{pmatrix} \pi/p & -\pi/2 \\ 0 & \pi/2 \end{pmatrix} \mathbb{Z}^2, & \text{if } k \in \{3p+1, \ldots, 6p\}. \end{cases}$$

Example C Let $\Lambda = \mathbb{Z}^2$ again and consider the case of the triadic (separable) MRA defined by

$$A_0 = \{\xi \in \mathbb{R}^2 : \ |\xi_1| < 2\pi/3 \ \text{ and } \ |\xi_2| < 2\pi/3\}$$

and

$$\Gamma_0 = 3\,\mathbb{Z}^2$$

We can obtain this time $8p$ directions (with $p \in \mathbb{N} \setminus \{0\}$) as it is shown Figure 2–C. Compared to the dyadic MRA, this construction permits to have a larger frequency support and, consequently, a better space localization in the direction of oscillations.

Example D Let $\Lambda = \mathbb{Z}^2$ and

$$A_0 = \{\xi \in \mathbb{R}^2 : \ |\xi_1| < \pi, \ |2\xi_1 + 3\xi_2| < 2\pi \ \text{ and } \ |2\xi_1 - 3\xi_2| < 2\pi\} \tag{9}$$

which is associated with the subsampling lattice

$$\Gamma_0 = \begin{pmatrix} 2 & 0 \\ 1 & 2 \end{pmatrix} \mathbb{Z}^2. \tag{10}$$

The boundary of this set A_0 is, in some sense, closer to a circle than the previous examples, although it is only invariant by rotation of π. As the lattice Γ_0 is not obtained from Λ by dilation and rotation, the same filter bank should not be used at the next level of the decomposition in order to keep the isotropy property. It can be replaced by a filter bank designed on the basis of the next example which deals with hexagonal MRA. The generated wavelets will not derived therefore from an MRA in a usual sense.

In this example, one can obtain 3 directions only. They are given by

$$\begin{array}{rcl} A_1 & = & \{\xi \in [-\pi, \pi]^2 \setminus A_0 : \ |\xi_2| \leq 2|\xi_1|/3\} \\ A_2 & = & \{\xi \in [-\pi, \pi]^2 \setminus A_0 : \ \xi_2 \leq 3\xi_1/2 \leq 0 \text{ or } 0 \leq 3\xi_1/2 \leq \xi_2\} \\ A_3 & = & \{\xi \in [-\pi, \pi]^2 \setminus A_0 : \ (-\xi_1, \xi_2) \in A_2\} \end{array} \tag{11}$$

(see Figure 2–D). However, if one allows some aliasing, it is possible to obtain $6p$ directions as it is shown Figure 3–D. Notice that the aliased areas are in the corners of the spectrum. Images concentrate generally very few energy on these regions since most optics have circulary symmetric lenses.

Example E The example of the hexagonal MRA is interesting as it allows to have a more isotropic refinement filter. (It is invariant by rotation of $\pi/3$.) The associated

directional filter banks generate therefore frequency partitionings that are closer to the ideal partitioning of Figure 1. Let

$$\Lambda = \begin{pmatrix} 1 & 0 \\ 1/\sqrt{3} & 2/\sqrt{3} \end{pmatrix} \mathbb{Z}^2,$$

with reciprocal lattice

$$\Lambda^* = \begin{pmatrix} 2\pi & -\pi \\ 0 & \sqrt{3}\pi \end{pmatrix} \mathbb{Z}^2.$$

Hence, the reciprocal cell is

$$\mathcal{C} = \{\xi \in \mathbb{R}^2 : \ |\xi_1| < \pi \ \& \ |\xi_1 + \sqrt{3}\xi_2| < \sqrt{3}\pi \ \& \ |\xi_1 + \sqrt{3}\xi_2| < \sqrt{3}\pi\}.$$

A natural choice for the refinement filter is given by

$$A_0 = \{\xi \in \mathbb{R}^2 : \ 2\xi \in \mathcal{C}\} \quad \text{and} \quad \Gamma_0 = 2\Lambda.$$

One can have $3p$ directions (with $p \in \mathbb{N} \setminus \{0\}$–see Figure 2–E) where the wavelet subbands are sampled on three different lattices that are obtained one from another by rotation of $\pm\pi/3$. For $p = 1$, one has $\Gamma_k = \Gamma_0$. It corresponds to the usual hexagonal wavelets [6].

When they are applied recursively, all these filter banks generate Shannon wavelets whose frequency supports are given on Figure 3. An anisotropy scaling law [4] can be prescribed to the generated basis as for curvelet and contourlet frames. It consists in doubling the number of directions when refining from coarse to fine (see Figure 3–B,C,D,E).

4 Regular 2-band filter banks

The bad localization in the space domain of Shannon wavelets is due to the lack of regularity of their Fourier transforms and of the transfer functions of the associated filter bank. The next sections are devoted to the construction of smooth approximations of the Shannon filters considered above. As regular M-band filter banks are difficult to obtain, their design is always limited to 2 bands. The smooth transfer functions will be constructed by products and sums of 2-band filters.

Given an original image defined on $\Lambda = \mathbb{Z}^2$, the two bands generated by perfect reconstruction quincunx filters $(Q_k, \widetilde{Q}_k)_{k\in\{0,1\}}$ are subsampled on the quincunx lattice $\Gamma = \mathrm{Q}\,\mathbb{Z}^2$ with sampling matrix

$$\mathrm{Q} = \begin{pmatrix} 1 & 1 \\ 1 & -1 \end{pmatrix}. \tag{12}$$

The design of these filters is restricted to Q_0 and $\widetilde{Q}_0$ since one sets, in practice, $Q_1(\xi) = e^{i\xi_1}\widetilde{Q}_0(\xi + (\pi,\pi))$ and $\widetilde{Q}_1(\xi) = e^{i\xi_1}Q_0(\xi + (\pi,\pi))$, $\forall \xi = (\xi_1,\xi_2) \in \mathbb{R}^2$. If

$$Q_0 = \widetilde{Q}_0 = \sqrt{2}\ \chi_{A_0 + 2\pi\mathbb{Z}^2},$$

the perfect reconstruction condition is satisfied if and only if $\{A_0, A_0 + (\pi,\pi)\}$ is a partition of $\mathbb{T}^2 = \mathbb{R}^2/\Lambda^*$. When Q_0 and $\widetilde{Q}_0$ are smooth, their energy is, in general, mostly concentrated on a set A_0 that satisfies the above condition and that we call

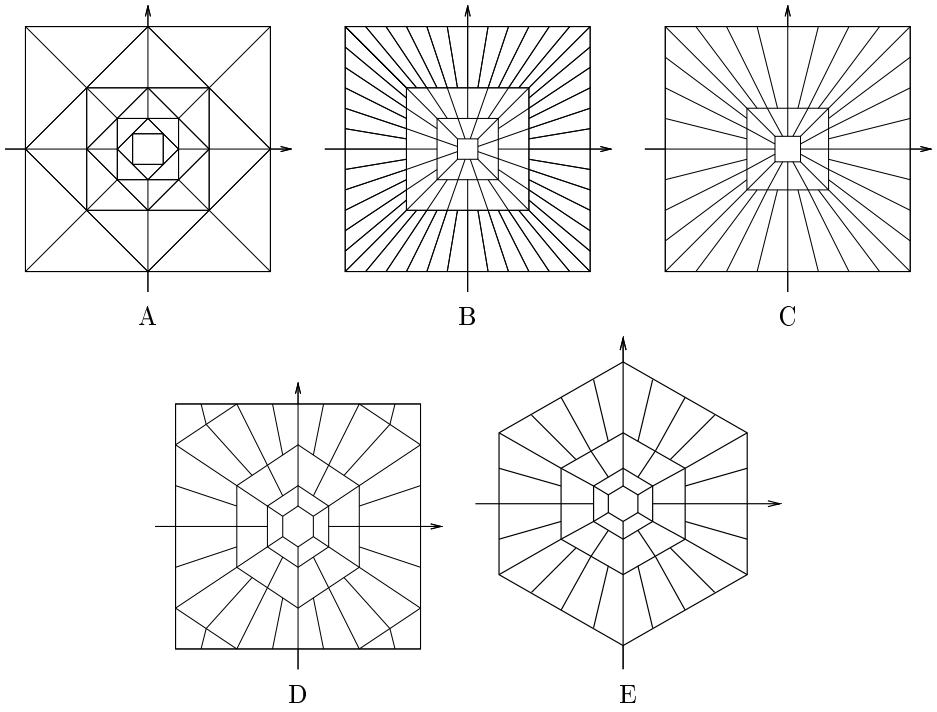

Figure 3: Examples of frequency supports of Shannon directional wavelets.

ideal support of Q_0 (and $\widetilde{Q}_0$). In order to obtain a regular filter whose support approximates the set A_0, put, for instance,

$$Q_0 = \widetilde{Q}_0 = \frac{\sqrt{2}\; g * \chi_{A_0+2\pi\mathbb{Z}^2}}{\left(\sum_{\gamma\in\Gamma^*/2\pi\mathbb{Z}^2} |g * \chi_{A_0+2\pi\mathbb{Z}^2}(\,.\,+\gamma)|^2\right)^{1/2}}, \tag{13}$$

where $\Gamma^*/2\pi\mathbb{Z}^2 = \{(0,0),(\pi,\pi)\}$ and $g \in C^\infty(\mathbb{R}^2)$ is non-negative and even. Notice that, for all $\epsilon > 0$ and all $p \geq 1$, there is a function g such that $\|Q_0 - \chi_{A_0}\|_p < \epsilon$. This remark will be used in Section 6. Transformation of variable (generalized McClellan transformation) [18] permits to get finite impulse response (FIR) biorthogonal filters having similar shape.

The most commonly used quincunx filters are diamond shaped filters that are characterized by the ideal support

$$\{\xi \in [-\pi,\pi]^2 :\ |\xi_1+\xi_2| < \pi \ \&\ |\xi_1-\xi_2| < \pi\} + 2\pi\mathbb{Z}^2$$

(see Figure 4–left). Symmetric (biorthogonal or infinite impulse response–IIR) diamond shape filters are usually designed from 1D filters using McClellan transformation [16]: if m_0 is a symmetric 1D filter with ideal support $[-\pi/2,\pi/2]+2\pi\mathbb{Z}$, write

$$m_0(\xi) = \mathcal{P}(\cos\xi), \quad \forall \xi \in \mathbb{R}.$$

Then put

$$Q_0(\xi) = \mathcal{P}\left(\frac{\cos\xi_1 + \cos\xi_2}{2}\right), \quad \forall \xi \in \mathbb{R}^2.$$

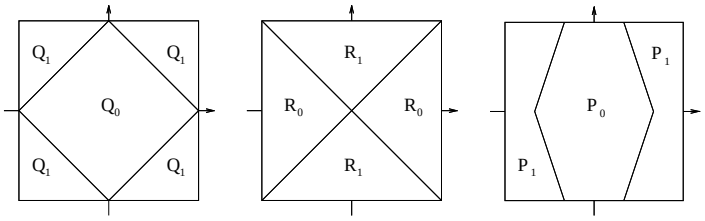

Figure 4: Ideal supports of (Q_0, Q_1), (R_0, R_1) and (P_0, P_1).

In the sequel, the notation $(Q_k, \tilde{Q}_k)_{k\in K}$ will be reserved for diamond shape filters.

We can also define $R_0(\xi) = Q_0(\xi + (\pi, 0))$ which is mostly supported on

$$\{\xi \in [-\pi, \pi]^2 : \ |\xi_1| > |\xi_2|\} + 2\pi\mathbb{Z}^2$$

(see Figure 4–middle). Notice that this kind of directional filters, known as fan filters, is already used in the contourlet transform.

We will also denote P_0 a regular filter whose support approximates the set

$$A_0 = \{\xi \in [-\pi, \pi]^2 : \ |3\xi_1 + \xi_2| < 2\pi \ \& \ |3\xi_1 - \xi_2| < 2\pi\} + 2\pi\mathbb{Z}^2$$

(see Figure 4–right). It can be design by generalized McClellan transform. The simplest way to approximate that support is indeed to write

$$P_0(\xi) = \mathcal{P}\left(\frac{2\cos\xi_1 + \cos\xi_2}{3}\right), \quad \forall \xi \in \mathbb{R}^2.$$

Quincunx filters are not the only 2-band filters on $l^2(\mathbb{Z}^2)$. Other sampling lattices are possible. Let us define $S_0(\xi) = Q_0(\mathrm{Q}\,\xi)$ (where Q is defined in (12)) with ideal support

$$\{\xi \in [-\pi, \pi]^2 : \ (|\xi_1| < \pi/2 \ \& \ |\xi_2| < \pi/2) \text{ or } (|\xi_1 > \pi/2 \ \& \ |\xi_2| > \pi/2)\} + 2\pi\mathbb{Z}^2$$

(see Figure 5–left) and

$$N_0(\xi) = Q_0\left(\mathrm{Q}\,\xi + (\pi, 0)\right) \tag{14}$$

with ideal support

$$\{\xi \in [-\pi, \pi]^2 : \ (\xi_1 > 0 \ \& \ \xi_2 > 0) \text{ or } (\xi_1 < 0 \ \& \ \xi_2 < 0)\} + 2\pi\mathbb{Z}^2$$

(see Figure 5–middle). These last two filter banks $(S_k, \widetilde{S}_k)_{k\in\{0,1\}}$ and $(N_k, \widetilde{N}_k)_{k\in\{0,1\}}$ are associated with the sampling lattice

$$\Gamma = \begin{pmatrix} 2 & 0 \\ 0 & 1 \end{pmatrix}\mathbb{Z}^2 \ \text{ or equivalently, } \ \Gamma = \begin{pmatrix} 1 & 0 \\ 0 & 2 \end{pmatrix}\mathbb{Z}^2.$$

Notice that when it is applied to the spaces $(V_j \otimes W_j)_j$, $(W_j \otimes V_j)_j$ and $(W_j \otimes W_j)_j$ generated by separable wavelets [14], the filter bank $(N_k, \widetilde{N}_k)_{k\in\{0,1\}}$ leads to the same frequency partitioning as complex wavelets [10] without redundancy (see Figure 6).

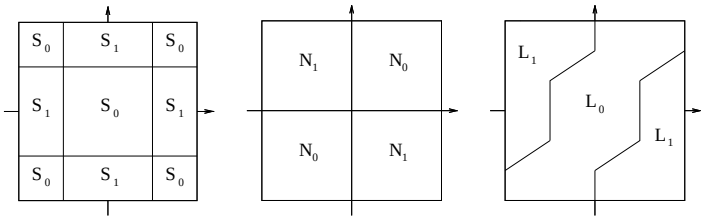

Figure 5: Ideal supports of (S_0, S_1), (N_0, N_1) and (L_0, L_1).

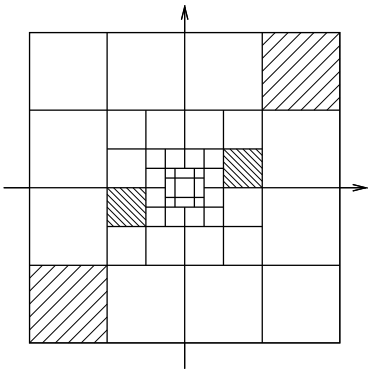

Figure 6: Frequency partitioning of complex wavelets.

Given 1D dyadic filters $(m_k, \widetilde{m}_k)_{k\in\{0,1\}}$, we can equivalently define

$$\begin{array}{rcl} M_0(\xi) & = & m_0(\xi_1)\, m_0(\xi_2), \\ M_1(\xi) & = & m_0(\xi_1)\, m_1(\xi_2)\, N_1(2\xi), \\ M_2(\xi) & = & m_0(\xi_1)\, m_1(\xi_2)\, N_0(2\xi), \\ M_3(\xi) & = & m_1(\xi_1)\, m_0(\xi_2)\, N_1(2\xi), \\ M_4(\xi) & = & m_1(\xi_1)\, m_0(\xi_2)\, N_0(2\xi), \\ M_5(\xi) & = & m_1(\xi_1)\, m_1(\xi_2)\, N_1(2\xi), \\ M_6(\xi) & = & m_1(\xi_1)\, m_1(\xi_2)\, N_0(2\xi), \end{array} \tag{15}$$

and define the same way the conjugate filters. This construction was suggested in [8] and developed independently by Lu and Do in [13].

Define also L_0 with ideal support $A_0 \cup A_2$ as defined in (9-11) (see Figure 5–right) and subsampling lattice

$$\Gamma = \begin{pmatrix} 2 & 0 \\ 0 & 1 \end{pmatrix} \mathbb{Z}^2.$$

It can be designed using (13) (changing A_0 in $A_0 \cup A_2$, and with $\Gamma^*/2\pi\mathbb{Z}^2 = \{(0,0), (\pi,0)\}$) or using [18].

At last, we will use filters $(\mathcal{N}_k, \widetilde{\mathcal{N}}_k)_{k\in\{0,1\}}$ that have the same geometry as $(N_k, \widetilde{N}_k)_{k\in\{0,1\}}$, but which satisfy the only constraints $\mathcal{N}_0\widetilde{\mathcal{N}}_0 + \mathcal{N}_1\widetilde{\mathcal{N}}_1 = 1$ and $\mathcal{N}_k(\,\cdot\,, (\pi,\pi)) = \mathcal{N}_k$, $\forall k \in \{0,1\}$. They can be obtained by putting, for example, $\mathcal{N}_k = N_k/\sqrt{2}$, but more degrees of freedom are possible in their design.

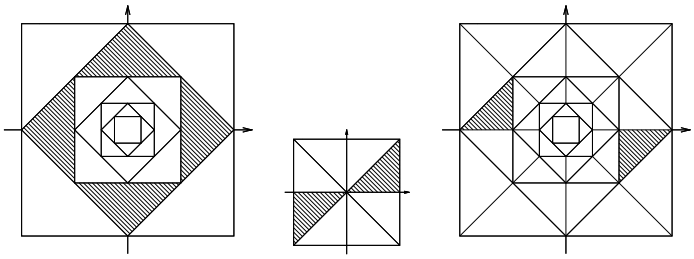

Figure 7: Ideal frequency supports of a quincunx wavelet, a directional filter and the obtained directional wavelet.

5 Quincunx directional wavelets (Example A)

The example of quincunx MRA is interesting as it uses, already implemented, diamond-shaped filters (and the associated fan filters) only. The obtained wavelets have however limited directionality. For 2 directions, put

$$\begin{aligned} M_0(\xi) &= Q_0(\xi), \\ M_1(\xi) &= Q_1(\xi)\, R_0(\mathrm{Q}\xi), \\ M_2(\xi) &= Q_1(\xi)\, R_1(\mathrm{Q}\xi), \end{aligned}$$

where the matrix Q and the functions Q_k and R_k are defined in the previous section. Define the same way the synthesis filters $\widetilde{M}_k$. This construction amounts to applying, first, the filters (Q_0, Q_1) (followed by the adapted subsampling), then to applying the filters (R_0, R_1) to the high frequency band. To obtain 4 directions, apply (R_0, R_1) twice (see Figure 7), or put equivalently,

$$\begin{aligned} M_0(\xi) &= Q_0(\xi), \\ M_1(\xi) &= Q_1(\xi)\, R_0(\mathrm{Q}\xi)\, R_0(\mathrm{Q}^2\xi), \\ M_2(\xi) &= Q_1(\xi)\, R_0(\mathrm{Q}\xi)\, R_1(\mathrm{Q}^2\xi), \\ M_3(\xi) &= Q_1(\xi)\, R_1(\mathrm{Q}\xi)\, R_1(\mathrm{Q}^2\xi), \\ M_4(\xi) &= Q_1(\xi)\, R_1(\mathrm{Q}\xi)\, R_0(\mathrm{Q}^2\xi). \end{aligned}$$

6 Dyadic directional wavelets with separable refinement filter (Example B)

The wavelets introduced in example B have the noteworthy property that they can be constructed from a separable MRA. The design and the regularity of separable MRA have already been widely studied. Moreover, the associated filters are implemented in faster algorithms.

For simplicity, we first consider the case of orthonormal wavelets or, in other words, the case when $\widetilde{M}_k = M_k$, $\forall k \in \{0, \ldots, 6\}$. In order to regularize the directional filters defined in Example B, it is not possible to use the same approach as Meyer wavelets (see [14]) as it is shown by the following proposition. Denote by $B(0, \epsilon)$ the unit ball of radius ϵ and by supp f the support of a function f.

Proposition 3 *Let $\epsilon \in (0, \pi/(6\sqrt{2}))$ and let the sets $\{A_k\}_{k\in\{0,\ldots,6\}}$ be defined by (6). There do not exist functions $(M_k)_{k\in\{0,\ldots,6\}}$ in $L^2(\mathbb{T}^2)$ such that the three following properties are satisfied simultaneously*

i) the matrix $|\Lambda/\Gamma|^{-1/2}M$ *is unitary,*

ii) the functions M_k *are continuous, for all* $k \in \{0, \ldots, 6\}$,

iii) their supports satisfy $\text{supp } M_k \subset A_k + B(0, \epsilon)$, *for all* $k \in \{0, \ldots, 6\}$.

This kind of property has already been considered as the permissibility condition [5]. One says that the passband supports of Figure 2–B are nonpermissible.

Proof. The idea of the proof is to show that the condition

$$\sum_{\gamma \in \Gamma^*/(\mathbb{Z}^2)^*} \overline{M_1(\,.\,+\gamma)} M_3(\,.\,+\gamma) = 0, \tag{16}$$

which is a consequence of *i)*, is in contradiction with *ii)* and *iii)* since, by the latter conditions, the terms of the sum (16) cannot cancel. Indeed, by condition *iii)*,

$$\text{supp } \overline{M_1} M_3 \subset E = ([-\pi, -\pi/3] \cup [\pi/3, \pi]) \times \{\pi\} + B(0, \epsilon) + 2\pi\,\mathbb{Z}^2.$$

Thus

$$\text{supp } \overline{M_1} M_3 \cap \text{supp } \overline{M_1(\,.\,+\gamma)} M_3(\,.\,+\gamma) = \emptyset, \quad \forall \gamma \in \Gamma^*/(\mathbb{Z}^2)^* \setminus \{(0,0), (\pi, 0)\}, \tag{17}$$

where Γ^* is defined by (8), while

$$\text{supp } \overline{M_1} M_3 \cap \text{supp } \overline{M_1(\,.\,+(\pi,0))} M_3(\,.\,+(\pi,0)) \subset F,$$

with

$$F = ([-2\pi/3, -\pi/3] \cup [\pi/3, 2\pi/3]) \times \{\pi\} + B(0, \epsilon) + 2\pi\,\mathbb{Z}^2.$$

Condition (16) implies therefore that $\text{supp } \overline{M_1} M_3 \subset F$. Put

$$G = \{\xi \in E \setminus F : \ \|\xi - \eta\| \geq \epsilon, \forall \eta \in A_i, \forall i \neq 1, 3\}.$$

As $\epsilon < \pi/(6\sqrt{2})$, the set G is non empty. Clearly, $M_i = 0$ on G, for $i \neq 1, 3$, and the condition $\sum_{i=0}^{6} |M_i|^2 = 1$ becomes $|M_1|^2 + |M_3|^2 = 1$ on G. Moreover, on the boundary of each connected component of G, there is a point ξ_1 such that $M_3(\xi_1) = 0$ and consequently $|M_1(\xi_1)| = 1$, and there is a point ξ_3 such that $M_1(\xi_3) = 0$ and $|M_3(\xi_3)| = 1$. This contradicts the fact that $\overline{M_1} M_3 = 0$ on G and M_1, M_3 are continuous. ◇

This proposition means that, in some sense, regularized filters have aliased components, and it can be seen as a drawback of the proposed transformation. We have however the following property.

Proposition 4 *Let* $\epsilon > 0$, $p \in [1, \infty)$ *and let the sets* $\{A_k\}_{k \in \{0,\ldots,6\}}$ *be defined by (6). There exist* $\{M_k\}_{k \in \{0,\ldots,6\}}$ *in* $L^2(\mathbb{T}^2)$ *such that*

i) the matrix $|\Lambda/\Gamma|^{-1/2}M$ *is unitary,*

ii) the functions M_k *are* C^∞, *for all* $k \in \{0, \ldots, 6\}$,

iii) we have $\| \, |M_k| - \chi_{A_k} \|_p < \epsilon$, *for all* $k \in \{0, \ldots, 6\}$.

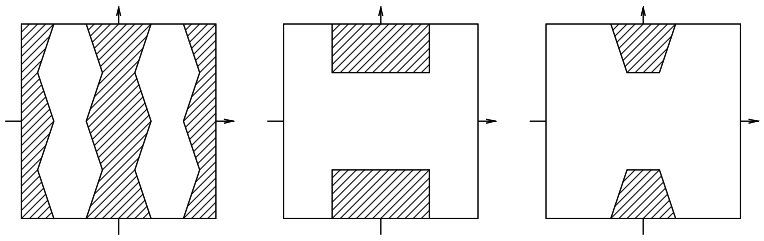

Figure 8: Ideal supports of $\xi \mapsto P_0(2\xi)$, $\xi \mapsto m_0(\xi_1)\, m_1(\xi_2)$ and $\xi \mapsto M_2(\xi)$.

A straightforward corollary of the proposition amounts to changing condition *iii)* into the weaker condition

$$\int_{A_k^c} |M_k(\xi)|^2 \, d\xi < \epsilon, \ \textit{for all } k \in \{0, \ldots, 6\},$$

where A_k^c is the complementary set of A_k in $[-\pi, \pi]^2$. It shows that the energy of M_k is mostly concentrated on A_k.

We give in the sequel a construction that can be used as a proof of the above proposition. Consider a separable MRA with 1-D quadrature mirror filters (m_0, m_1). Going back to (15), and changing (N_0, N_1) in (R_0, R_1) or (P_0, P_1), we clearly obtain new, perfect reconstruction, filter banks. Think , for instance, at

$$\begin{array}{rcl} M_0(\xi) & = & m_0(\xi_1)\, m_0(\xi_2), \\ M_1(\xi) & = & m_0(\xi_1)\, m_1(\xi_2)\, P_1(2\xi), \\ M_2(\xi) & = & m_0(\xi_1)\, m_1(\xi_2)\, P_0(2\xi), \\ M_3(\xi) & = & m_1(\xi_1)\, m_0(\xi_2)\, P_1(2\xi), \\ M_4(\xi) & = & m_1(\xi_1)\, m_0(\xi_2)\, P_0(2\xi), \\ M_5(\xi) & = & m_1(\xi_1)\, m_1(\xi_2)\, R_1(2\xi), \\ M_6(\xi) & = & m_1(\xi_1)\, m_1(\xi_2)\, R_0(2\xi). \end{array} \tag{18}$$

This filter bank does not corresponds to the sought frequency partitioning. However, using the filters $(\mathcal{N}_0, \mathcal{N}_1)$, we can also define

$$\begin{array}{rcl} M_0(\xi) & = & m_0(\xi_1)\, m_0(\xi_2), \\ M_1(\xi) & = & m_1(\xi_1)\, m_1(\xi_2)\, R_0(2\xi)\, \mathcal{N}_1(2\xi) + m_0(\xi_1)\, m_1(\xi_2)\, P_1(2\xi)\, \mathcal{N}_0(2\xi), \\ M_2(\xi) & = & m_0(\xi_1)\, m_1(\xi_2)\, P_0(2\xi), \\ M_3(\xi) & = & m_0(\xi_1)\, m_1(\xi_2)\, P_1(2\xi)\, \overline{\mathcal{N}_1(2\xi)} - m_1(\xi_1)\, m_1(\xi_2)\, R_0(2\xi)\, \overline{\mathcal{N}_0(2\xi)}, \\ M_4(\xi) & = & m_1(\xi_1)\, m_1(\xi_2)\, R_1(2\xi)\, \mathcal{N}_0(2\xi) + m_1(\xi_1)\, m_0(\xi_2)\, P_0(2\xi)\, \mathcal{N}_1(2\xi), \\ M_5(\xi) & = & m_1(\xi_1)\, m_0(\xi_2)\, P_1(2\xi), \\ M_6(\xi) & = & m_1(\xi_1)\, m_0(\xi_2)\, P_0(2\xi)\, \overline{\mathcal{N}_0(2\xi)} - m_1(\xi_1)\, m_1(\xi_2)\, R_1(2\xi)\, \overline{\mathcal{N}_1(2\xi)}. \end{array} \tag{19}$$

Notice that, for all k, the energy of M_k is mostly Concentrated on A_k as it is illustrated by the example given on Figure 8. The modulus of these functions can be arbitrarily close to the corresponding Shannon filters in the sense of the L^p-norm, since the associated two-band filters satisfy this property. Moreover, we have the following result.

Lemma 1 *The filter bank defined by (19) performs a perfect reconstruction.*

Proof. The matrix $|\Lambda/\Gamma|^{-1/2}M$ defined by (2) and (19) is unitary. Indeed, to prove that

$$\sum_{\gamma\in\Gamma^*/(\mathbb{Z}^2)^*} \overline{M_k(\xi+\gamma)}\, M_l(\xi+\gamma) = 8\,\delta_{kl}, \quad \forall k,l\in\{1,\ldots,6\} \tag{20}$$

notice that $\mathcal{N}_k(2\xi) = \mathcal{N}_k(2(\xi+\gamma))$, for all $\gamma\in\Gamma^*/(\mathbb{Z}^2)^*$ and $k\in\{0,1\}$. Factorize with $\mathcal{N}_k(2\xi)$, then use

$$|\mathcal{N}_0(\xi)|^2 + |\mathcal{N}_1(\xi)|^2 = 1$$

and the orthogonality of the filter bank defined by (18). This orthogonality is a straightforward consequence of

$$\overline{m_k(\xi_j)}\, m_l(\xi_j) + \overline{m_k(\xi_j+\pi)}\, m_l(\xi_j+\pi) = 2\,\delta_{kl}, \quad \forall k,l\in\{0,1\}, \forall j\in\{1,2\}$$

and

$$\overline{T_k(\xi)}\, T_l(\xi) + \overline{T_k(\xi+(\pi,\pi))}\, T_l(\xi+(\pi,\pi)) = 2\,\delta_{kl}, \quad \forall k,l\in\{0,1\},$$

where T stands for P or Q. When k or $l=0$, change M_0 in $M_0\, e^{i\langle\eta,\,\cdot\,\rangle}$ with $\eta=(0,0)$ or $(1,1)$, in (20). ◇

The technique used in the design of this filter bank could be developed in a more general form that include the method introduced by Maas [15] and Ayache [1] for the design of nonseparable filters.

More directions are generated by applying specially designed filters to each wavelet subband. These filters are obtained by combining some linear operators with N_0, N_1, P_0 or P_1. By this construction, we can have orthonormal bases for $L^2(\mathbb{R}^2)$ where the wavelets have fast decay. Using FIR filters, we get compactly supported wavelets having at least the same regularity and the same number of directional vanishing moments as the separable wavelets generated by (m_0, m_1). Notice indeed that these directional wavelets are finite sums of separable wavelets.

The method can be generalized to biorthogonal filters in order to have Riesz bases for $L^2(\mathbb{R}^2)$. Indeed, consider the filter bank

$$\begin{aligned}
M_0(\xi) &= m_0(\xi_1)\, m_0(\xi_2),\\
M_1(\xi) &= m_1(\xi_1)\, m_1(\xi_2)\, R_0(2\xi)\widetilde{\mathcal{N}}_1(2\xi) + m_0(\xi_1)\, m_1(\xi_2)\, P_1(2\xi)\mathcal{N}_0(2\xi),\\
M_2(\xi) &= m_0(\xi_1)\, m_1(\xi_2)\, P_0(2\xi),\\
M_3(\xi) &= m_0(\xi_1)\, m_1(\xi_2)\, P_1(2\xi)\overline{\mathcal{N}_1(2\xi)} - m_1(\xi_1)\, m_1(\xi_2)\, R_0(2\xi)\overline{\widetilde{\mathcal{N}}_0(2\xi)},\\
M_4(\xi) &= m_1(\xi_1)\, m_1(\xi_2)\, R_1(2\xi)\widetilde{\mathcal{N}}_0(2\xi) + m_1(\xi_1)\, m_0(\xi_2)\, P_0(2\xi)\mathcal{N}_1(2\xi),\\
M_5(\xi) &= m_1(\xi_1)\, m_0(\xi_2)\, P_1(2\xi),\\
M_6(\xi) &= m_1(\xi_1)\, m_0(\xi_2)\, P_0(2\xi)\overline{\mathcal{N}_0(2\xi)} - m_1(\xi_1)\, m_1(\xi_2)\, R_1(2\xi)\overline{\widetilde{\mathcal{N}}_1(2\xi)},
\end{aligned}$$

and

$$\begin{aligned}
\widetilde{M}_0(\xi) &= \widetilde{m}_0(\xi_1)\, \widetilde{m}_0(\xi_2),\\
\widetilde{M}_1(\xi) &= \widetilde{m}_1(\xi_1)\, \widetilde{m}_1(\xi_2)\, \widetilde{R}_0(2\xi)\mathcal{N}_1(2\xi) + \widetilde{m}_0(\xi_1)\, \widetilde{m}_1(\xi_2)\, \widetilde{P}_1(2\xi)\widetilde{\mathcal{N}}_0(2\xi),\\
\widetilde{M}_2(\xi) &= \widetilde{m}_0(\xi_1)\, \widetilde{m}_1(\xi_2)\, \widetilde{P}_0(2\xi),\\
\widetilde{M}_3(\xi) &= \widetilde{m}_0(\xi_1)\, \widetilde{m}_1(\xi_2)\, \widetilde{P}_1(2\xi)\overline{\widetilde{\mathcal{N}}_1(2\xi)} - \widetilde{m}_1(\xi_1)\, \widetilde{m}_1(\xi_2)\, \widetilde{R}_0(2\xi)\overline{\mathcal{N}_0(2\xi)},\\
\widetilde{M}_4(\xi) &= \widetilde{m}_1(\xi_1)\, \widetilde{m}_1(\xi_2)\, \widetilde{R}_1(2\xi)\mathcal{N}_0(2\xi) + \widetilde{m}_1(\xi_1)\, \widetilde{m}_0(\xi_2)\, \widetilde{P}_0(2\xi)\widetilde{\mathcal{N}}_1(2\xi),\\
\widetilde{M}_5(\xi) &= \widetilde{m}_1(\xi_1)\, \widetilde{m}_0(\xi_2)\, \widetilde{P}_1(2\xi),\\
\widetilde{M}_6(\xi) &= \widetilde{m}_1(\xi_1)\, \widetilde{m}_0(\xi_2)\, \widetilde{P}_0(2\xi)\overline{\widetilde{\mathcal{N}}_0(2\xi)} - \widetilde{m}_1(\xi_1)\, \widetilde{m}_1(\xi_2)\, \widetilde{R}_1(2\xi)\overline{\mathcal{N}_1(2\xi)}.
\end{aligned}$$

The same kind of arguments as above proves that it performs a perfect reconstruction.

7 Dyadic directional wavelets with hexagonal refinement filter (Example D)

The hexagonal MRA has several advantages on the square MRA. First, hexagonal lattices satisfy some interesting mathematical properties: they permit to avoid some connectivity problems that arise on square lattices, and they require the least number of samples to represent images with circulary spectrum. It is also possible to design refinement filters that are invariant by rotation of $\pi/3$. Moreover the number of wavelets can be restricted to 3 directions, and in such a case, we will show that the aliasing phenomenon revealed by Proposition 3 can be alleviated.

Since images are generally defined on square lattices, we consider Example D instead of Example E. Notice that these two transformations have the drawback of using nonseparable refinement filters. Once again, we consider the case of orthonormal wavelets, although the extension to biorthogonal wavelets is straightforward.

The partitioning of Figure 2-D can be achieved using the same technique as in Section 6. Put, for instance,

$$\begin{array}{rcl} M_0(\xi) & = & P_0(\xi_2, 2\xi_1)\, m_0(\xi_1), \\ M_1(\xi) & = & P_0(\xi_2, 2\xi_1)\, m_1(\xi_1), \\ M_2(\xi) & = & P_1(\xi_2, 2\xi_1)\, (\mathcal{N}_0(2\xi_1, \xi_2)\, m_0(\xi_1) + \overline{\mathcal{N}_1(2\xi_1, \xi_2)}\, m_1(\xi_1)), \\ M_3(\xi) & = & P_1(2\xi_2, \xi_1)\, (\overline{\mathcal{N}_0(2\xi_1, \xi_2)}\, m_0(\xi_1) - \mathcal{N}_0(2\xi_1, \xi_2)\, m_1(\xi_1)). \end{array}$$

In order to reduce the aliasing alluded above, one can also define

$$\begin{array}{rcl} M_0(\xi) & = & L_0(\xi)\, L_0(-\xi_1, \xi_2), \\ M_1(\xi) & = & L_1(\xi)\, L_1(-\xi_1, \xi_2), \\ M_2(\xi) & = & L_0(\xi)\, L_1(-\xi_1, \xi_2), \\ M_3(\xi) & = & L_1(\xi)\, L_0(-\xi_1, \xi_2). \end{array}$$

One obtains 6 directions by using the filters (N_0, N_1). For instance, apply $\xi \mapsto N_0(\xi_1, \xi_2/2)$ to the 1^{st} wavelet subband (see Figure 9–left). Equivalently, define

$$\begin{array}{rcl} M_0(\xi) & = & L_0(\xi)\, L_0(-\xi_1, \xi_2), \\ M_1(\xi) & = & L_1(\xi)\, L_1(-\xi_1, \xi_2)\, N_0(2\xi_1, \xi_2), \\ M_2(\xi) & = & L_1(\xi)\, L_1(-\xi_1, \xi_2)\, N_1(2\xi_1, \xi_2), \\ M_3(\xi) & = & L_0(\xi)\, L_1(-\xi_1, \xi_2)\, N_0(\mathrm{D}_1\xi), \\ M_4(\xi) & = & L_0(\xi)\, L_1(-\xi_1, \xi_2)\, N_1(\mathrm{D}_1\xi), \\ M_5(\xi) & = & L_1(\xi)\, L_0(-\xi_1, \xi_2)\, N_0(\mathrm{D}_2\xi), \\ M_6(\xi) & = & L_1(\xi)\, L_0(-\xi_1, \xi_2)\, N_1(\mathrm{D}_2\xi), \end{array}$$

where

$$D_1 = \begin{pmatrix} 1 & 3/2 \\ -1 & 1/2 \end{pmatrix} \quad \text{and} \quad D_2 = \begin{pmatrix} -1 & 3/2 \\ -1 & -1/2 \end{pmatrix}.$$

As in section 6, more directions are obtained by applying filter bancs that are designed by combining well adapted linear operators with (P_0, P_1) or (N_0, N_1) (see Figure 9).

By (10), at the next levels of the pyramidal algorithm, original lattices are

$$\Lambda = 2^j \begin{pmatrix} 1 & 0 \\ 1/2 & 1 \end{pmatrix} \mathbb{Z}^2, \quad \text{for } j \geq 1.$$

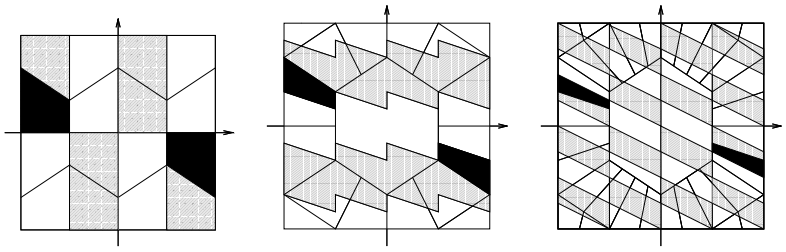

Figure 9: Ideal supports of $\xi \mapsto N_0(2\xi_1, \xi_2)$, $P_1 \circ F$ and $N_0 \circ G$ for two linear operators F and E.

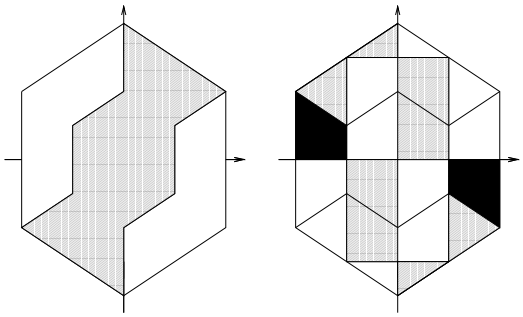

Figure 10: Ideal supports of $\xi \mapsto P_0(\mathrm{E}\xi)$ and $\xi \mapsto N_0(2\xi_1, \xi_2)$.

By a change of scale, they come down to the case $j = 0$. In other words,

$$\Lambda = \begin{pmatrix} 1 & 0 \\ 1/2 & 1 \end{pmatrix} \mathbb{Z}^2 \quad \text{and} \quad \Lambda^* = \begin{pmatrix} 2\pi & \pi \\ 0 & 2\pi \end{pmatrix} \mathbb{Z}^2.$$

One can distort hexagonal filters [6] to obtain 3 directions. Since the lattice is not invariant by rotation of $\pi/3$, one does not need to design filters that satisfy this invariance property. Therefore, we can use (see Figure 10–left)

$$\begin{aligned} M_0(\xi) &= P_0(\mathrm{E}\,\xi)\, P_0(\mathrm{E}(-\xi_1, \xi_2)), \\ M_1(\xi) &= P_1(\mathrm{E}\,\xi)\, P_1(\mathrm{E}(-\xi_1, \xi_2)), \\ M_2(\xi) &= P_0(\mathrm{E}\,\xi)\, P_1(\mathrm{E}(-\xi_1, \xi_2)), \\ M_3(\xi) &= P_1(\mathrm{E}\,\xi)\, P_0(\mathrm{E}(-\xi_1, \xi_2)), \end{aligned}$$

where

$$\mathrm{E} = \begin{pmatrix} 1 & -1/2 \\ 1 & 3/2 \end{pmatrix}.$$

Once again, more directions are obtained by using (N_0, N_1) (see Figure 10–right) and (P_0, P_1). More precisely, for 6 directions, let

$$\begin{aligned} M_0(\xi) &= P_0(\mathrm{E}\,\xi)\, P_0(\mathrm{E}(-\xi_1, \xi_2)), \\ M_1(\xi) &= P_1(\mathrm{E}\,\xi)\, P_1(\mathrm{E}(-\xi_1, \xi_2))\, N_0(2\xi_1, \xi_2), \\ M_2(\xi) &= P_1(\mathrm{E}\,\xi)\, P_1(\mathrm{E}(-\xi_1, \xi_2))\, N_1(2\xi_1, \xi_2), \\ M_3(\xi) &= P_0(\mathrm{E}\,\xi)\, P_1(\mathrm{E}(-\xi_1, \xi_2))\, N_0(\mathrm{D}_1\xi), \\ M_4(\xi) &= P_0(\mathrm{E}\,\xi)\, P_1(\mathrm{E}(-\xi_1, \xi_2))\, N_1(\mathrm{D}_1\xi), \\ M_5(\xi) &= P_1(\mathrm{E}\,\xi)\, P_0(\mathrm{E}(-\xi_1, \xi_2))\, N_0(\mathrm{D}_2\xi), \\ M_6(\xi) &= P_1(\mathrm{E}\,\xi)\, P_0(\mathrm{E}(-\xi_1, \xi_2))\, N_1(\mathrm{D}_2\xi). \end{aligned}$$

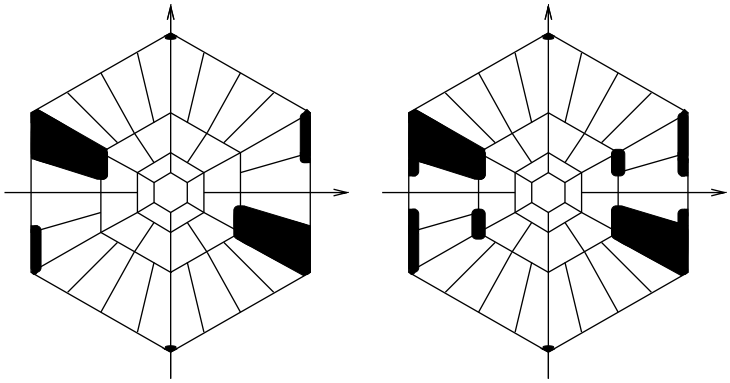

Figure 11: Ideal (left) and real (right) frequency support of a passband directional filter.

As it is mentioned above, Proposition 3 does not extend to the proposed frequency partitioning (and the associated partitioning of Example E) in the case of 3 directions. To obtain a counterexample, put

$$M_0 = \frac{2\, g * \chi_{A_0+\Lambda^*}}{\left(\sum_{\gamma\in\Gamma^*/\Lambda^*} |g * \chi_{A_0+\Lambda^*}(\,.\,+\gamma)|^2\right)^{1/2}}, \tag{21}$$

where A_0 is defined by (9), $\Gamma^*/\Lambda^* = \{(0,0),(\pi,0),(\pi/2,\pi),(-\pi/2,\pi)\}$ and $g \in C^\infty(\mathbb{R}^2)$ is non-negative, even and such that supp $g \subset B(0,\epsilon)$. Clearly M_0 is supported on $A_0 + B(0,\epsilon) + \Lambda^*$. (One can also define $M_0(\xi) = S_0(\xi_1,\xi_2)\, P_0(\xi_2, 2\xi_1)$ where S_0 and P_0 are well localized.) As M_0 is real-valued, the wavelet filters can be defined by

$$\begin{aligned} M_1(\xi) &= e^{i(\xi_1-\xi_2/2)}\, M_0(\xi+(\pi,0)), \\ M_2(\xi) &= e^{i(\xi_1+\xi_2/2)}\, M_0(\xi+(\pi/2,\pi)), \\ M_3(\xi) &= e^{i\xi_2}\, M_0(\xi+(-\pi/2,\pi)). \end{aligned}$$

One checks easily that the so defined matrix $2^{-1}\,(M_k(\xi+\gamma))_{k\in\{0,\ldots,3\};\gamma\in\Gamma^*/\Lambda^*}$ is unitary.

Unfortunately, this result does not extend to the case of 6 directions (or 6×2^p directions, more generally). Indeed, in order to show that the passband support of the filters are nonpermissible, one can adapt the proof of Proposition 3 to the sets A_1 and A_2 of Figure 2-E, for instance. However we can design filters that have very few aliasing by using (N_0, N_1) that are obtained by (13-14). For more directions, use again (N_0, N_1) and (P_0, P_1) designed by the same method (see Figure 9 and Figure 11).

References

[1] A. Ayache, "Construction of non separable dyadic compactly supported orthonormal wavelet bases for $L^2(R^2)$ of arbitrarily high regularity", Revista Matematica Iberoamericana, 15(1):37–58, 1999.

[2] E. J. Candès and D. L. Donoho, "Ridgelets – a key to higher dimensional intermittency ?", Phil. Trans. R. Soc. Lond. A., pp:2495–2509, 1999.

[3] E. J. Candès and D. L. Donoho, "Curvelets – a suprizingly effective nonadaptive representation for objects with edges", Curve and Surface Fitting, Vanderbuilt Univ. Press, 1999.

[4] E. J. Candès and D. L. Donoho, "Curvelets – Multiresolution representation and scaling laws", SPIE Wavelet Applications in Signal and Image Processing VIII, Vol. 4119, 2000.

[5] T. Chen and P. Vaidyanathan, "Considerations in multidimensional filter bank design", in Proc. of IEEE Int. Symp. on Circuits and Systems, 643–645, 1993.

[6] A. Cohen and J. M. Schlenker, "Compactly supported bidimensional wavelet bases with hexagonal symmetry", Constructive Approximation, 9:209–236, 1993.

[7] M. N. Do and M. Vetterli, "Contourlets", Beyond Wavelets, Academic Press, New York, 2003.

[8] S. Durand, "Orthonormal bases of non-separable wavelets with shrap directions", in proc. IEEE Int. Conf. on Image Proc., 2005.

[9] P. Hong and J. T. Smith, "An octave-band family of non-redundant directional filter banks", in proc. IEEE Int. Conf. on Acoust. Speech and Signal Proc., 2002.

[10] N. G. Kingsbury, "The dual-tree complex wavelet transform: A new technique for shift invariance and directional filters", in proc. IEEE DSP, 1998.

[11] E. Le Pennec and S. Mallat, "Sparse geometrical image representation with bandelets", IEEE Trans. on Image Processing, 2004.

[12] Y. Lu and M. N. Do, "CRIPS-contourlets: a critical sampled directional multiresolution image representation", in proc. SPIE Conf. on Wavelet Applic. in Signal and Image Proc., San Diego, 2003.

[13] Y. Lu and M. N. Do, "The finer directional wavelet transform", in proc. IEEE Int. Conf. on Acoust. and Signal Proc., 2005.

[14] S. Mallat, "A Wavelet Tour of Signal Processing", Academic Press, London, 1999.

[15] P. Maass, "Families of orthogonal two-dimensional wavelets", SIAM J. Math. Anal., 27:1454–1481, 1996.

[16] J. H. McClellan, "The design of two-dimensional digital filters by transformations", in proc. 7^{th} Annual Princeton Conf. Inf. Sciences and Systems, 1973.

[17] T. T. Nguyen and S. Oraintara, "Multiresolution Direction Filter Banks: Theory, Design and Applications", IEEE Trans. Signal Proc., 3895–3905, 2005.

[18] D. B. H. Tay and N. Kingsbury, "Flexible design of multidimensional perfect reconstruction FIR 2-band filters using transformations of variables", IEEE Trans. Image Proc. 2:466–480, 1993.

[19] M. Vetterli, "Filter bank allowing perfect reconstruction", Signal Processing, 10: 219–244, 1986.